Physics Procedia

Volume 75, 2015, Pages 121–126

20th International Conference on Magnetism

Anisotropic Chemical Pressure Effect on the Antiferromagnetic Kondo Semiconductor $Ce(Ru_{1-x}Fe_x)_2Al_{10}$

Kyosuke Hayashi[1*], Yuji Muro[1†], Tadashi Fukuhara[1], Tomohiko Kuwai[2], Jo Kawabata[3], Toshiro Takabatake[3,4], Masato Hagihala[5] and Kiyoichiro Motoya[5]

[1]*Faculty of Engineering, Toyama Prefectural University, Imizu 939-0398, Japan*
[2]*Graduate School of Science and Engineering, University of Toyama, Toyama 930-8555, Japan*
[3]*Dept. Quantum Matter, AdSM, and* [4]*IAMR, Hiroshima University, Higashi-Hiroshima 739-8530, Japan*
[5]*Dept. Physics, Faculty of Science and Technology, Tokyo University of Science, Noda 278-8510, Japan*
ymuro@pu-toyama.ac.jp

Abstract

We have studied the Fe substitution effect on the anomalous antiferromagnetic (AFM) order in $CeRu_2Al_{10}$ by using both single- and poly-crystalline samples. Electron probe microanalysis revealed that the single crystals of $Ce(Ru_{1-x}Fe_x)_2Al_{10}$ with $0.5 \leq x \leq 0.8$, grown by an Al self flux method, separate into Ru-rich central part and Fe-rich surface part. On the other hand, the composition in the polycrystalline samples is homogeneous. The magnetic susceptibility, electrical resistivity and specific heat measurements on the polycrystals indicate that T_N gradually decreases and disappears at $x = 0.7$. This is contrasting to the pressure induced peaking of T_N at 2.5 GPa. We should remind that application of hydrostatic pressure and Fe substitution result in different lattice contractions. The rate of contraction by the hydrostatic pressure is almost isotropic up to $P_c = 4$ GPa, while that by Fe substitution is strongly anisotropic; $\Delta a/a \approx \Delta c/c \approx 2\Delta b/b$. Therefore, the contrasting changes of T_N by Fe substitution and by hydrostatic pressure suggest that the degree of *c-f* hybridization along the *b*-axis controls the anomalous AFM order in $CeRu_2Al_{10}$.

Keywords: Kondo semiconductor, $CeRu_2Al_{10}$, substitution, chemical pressure effect

[*] Present address: Dept. Quantum Matter, AdSM, Hiroshima University, Higashi-Hiroshima 739-8530, Japan.
[†] Corresponding author.

Selection and peer-review under responsibility of the Scientific Programme Committee of ICM 2015

doi:10.1016/j.phpro.2015.12.017

1 Introduction

Since the first report on the anomalous magnetic and transport properties of the ternary Ce compound $CeRu_2Al_{10}$ [1], much experimental and theoretical efforts have been made to clarify the enigmatic antiferromagnetic (AFM) transition occurring at T_N = 27 K [2-5]. This compound, crystallizing in the orthorhombic $YbFe_2Al_{10}$ type structure [6], is a rare example of Kondo semiconductors showing the AFM order. The questions for $CeRu_2Al_{10}$ are not only the unusually high T_N which exceeds that of Gd counterpart (T_N = 15.5 K [7]), but also the maximum in T_N induced by pressure and substitution of Fe for Ru [2,8-10]. To explain these facts, an itinerant AFM state on the Kondo-Heisenberg model was proposed [11], which was used to understand the resonant x-ray emission data on $Ce(Ru_{1-x}Fe_x)_2Al_{10}$ [12]. In the μSR and neutron diffraction study using polycrystalline $Ce(Ru_{1-x}Fe_x)_2Al_{10}$, however, the x dependence of T_N deviates from the result on the single crystal study at $x \geq 0.5$ [13]. This discrepancy motivated us to reinvestigate the alloy system $Ce(Ru_{1-x}Fe_x)_2Al_{10}$ including careful characterization of samples. In this study, we analyzed the atomic composition of single-crystalline $Ce(Ru_{1-x}Fe_x)_2Al_{10}$ samples used for the previous study [10]. In addition, we measured the magnetic susceptibility, electrical resistivity and specific heat of polycrystalline $Ce(Ru_{1-x}Fe_x)_2Al_{10}$ for $0.5 \leq x \leq 0.8$, then compared the obtained x dependence of T_N to the reported pressure dependence of T_N in $CeRu_2Al_{10}$ [2,8].

2 Experimental

Polycrystalline samples of $Ce(Ru_{1-x}Fe_x)_2Al_{10}$ were synthesized by arc-melting the constituent amount of pure elements under an argon atmosphere. The obtained samples were annealed at 800 ºC one week. Single crystals were grown from pre-melted $Ce(Ru_{1-x}Fe_x)_2$ alloys and excess Al flux, details of which are described in the previous report [10]. The chemical composition of each sample was determined by the wave dispersion x-ray spectroscopy coupled to JEOL JXA-8100 electron-probe microanalyzer (EPMA) for single crystals and energy dispersion spectrometer (EDS) equipped on HITACHI S-3000N scanning electron microscope for polycrystals.

The magnetic susceptibility, χ, was measured by using a commercial SQUID magnetometer (Quantum Design MPMS) in B = 1 T. Measurements of electrical resistivity, ρ, were performed by using a dc four-probe method in the temperature range 0.5 K < T < 300 K. The specific heat, C, was measured by the relaxation method in a Quantum Design PPMS.

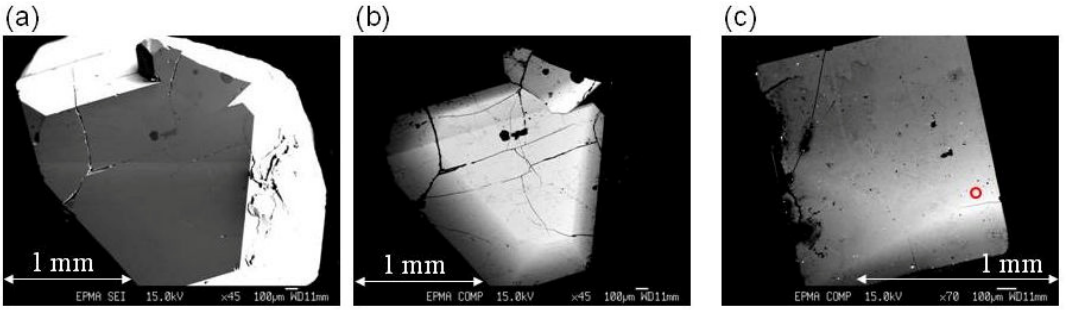

Figure 1: (a) Secondary electron and (b) backscattered electron images for single-crystalline $Ce(Ru_{0.5}Fe_{0.5})_2Al_{10}$. (c) Backscattered image for $Ce(Ru_{0.4}Fe_{0.6})_2Al_{10}$. A circle represents the area where x ~ 0.4.

3 Results and Discussion

3.1 Sample characterization of single crystals

Figure 1 shows (a) secondary-electron (SE) and (b) back-scattered electron (BSE) images of single-crystalline $Ce(Ru_{1-x}Fe_x)_2Al_{10}$ with nominal x = 0.5. A dark gray area in the SE image is a polished (010) facet. In spite of a flat surface, the BSE image shows a clear contrast between light and shade within the facet. Because the BSE image becomes more blight where the average atomic number of composed elements is higher, the contrast in Fig. 1(b) indicates the occurrence of phase segregation in a single crystal although we used pre-melted $Ce(Ru_{1-x}Fe_x)_2$ alloys for the flux growth. The quantitative analyses revealed that the Fe concentration x is ~ 0.6 for the light area in Fig. 1(b) while x ~ 0.8 for the shaded one. We also confirmed the homogeneity of Ce and Al over the all analyzed points of each crystal. Therefore, our EPMA on single crystals indicates that the Fe atoms in $Ce(Ru_{1-x}Fe_x)_2Al_{10}$ segregate to the surface of a crystal. The value of x in the light area exceeds the nominal value, which should be due to the existence of Ru rich part at the center of the crystal. Indeed, at the light area on the BSE image for a crystal with nominal x = 0.6 shown in Fig. 1(c), we obtained the value x ~ 0.4. The phase segregation was observed in all measured crystals in the range $0.5 \leq x \leq 0.8$. Thus, in order to proceed the measurements with single-crystalline $Ce(Ru_{1-x}Fe_x)_2Al_{10}$, we need to improve the technique of single crystal growth of $Ce(Ru_{1-x}Fe_x)_2Al_{10}$ to prevent the phase segregation.

3.2 Physical property of polycrystals

We confirmed the agreement between the nominal and analyzed compositions as well as the homogeneous mixture of Ru and Fe for the polycrystals, on which we carried out the measurements of χ, ρ and C. Figure 2(a) shows the inverse magnetic susceptibility, $1/\chi$, of polycrystalline $Ce(Ru_{1-x}Fe_x)_2Al_{10}$. All samples obey the Curie-Weiss law between 300 K and 100 K and show a broad peak in χ due to Kondo effect at low temperatures. The slope of $1/\chi$ should depend on the preferred orientation of polycrystalline samples because of the strong magnetic anisotropy $\chi_a > \chi_c > \chi_b$ observed in $CeRu_2Al_{10}$. With increasing x, the gradual increases of the temperature at the maximum in $\chi(T)$ indicates the enhancement of Kondo coupling that is also reported in the previous single-crystal studies [9,10].

Figure 2(b) displays the results of $\rho(T)$ normalized by ρ(300 K), ρ/ρ_{300}, for x = 0, 0.5, 0.6, 0.7 and 1. For x = 0.5, the disappearance of the maximum and continuous increase in ρ on cooling below 40 K to 5 K is similar to those observed in single-crystalline $Ce(Ru_{1-x}Fe_x)_2Al_{10}$ with x = 0.625 and $CeRu_2Al_{10}$ under P = 3 GPa [2,9]. At $x \geq 0.6$, the semiconducting behavior observed between 70 K and 30 K for x = 0 disappears then a maximum due to Kondo coherence appears at x = 0.7. No anomalies indicating the phase transitions were observed for x = 0.7 down to 0.5 K.

The results of C for $Ce(Ru_{1-x}Fe_x)_2Al_{10}$ at T < 40 K are shown in Fig. 2(c). In x = 0.5 and 0.6, a broadened C/T jump due to an AFM transition is observed at 22 K and 17 K, respectively. Above 30 K, the C/T values agree among x = 0, 0.5 and 0.6, in which the AFM transition occurs. The decrease in C/T for x = 0.7 means that the system changes to the mixed-valence regime.

Figure 2(d) shows the x dependence of T_N for polycrystalline $Ce(Ru_{1-x}Fe_x)_2Al_{10}$ in addition to the P-T phase diagram of $CeRu_2Al_{10}$ [2,8]. The values of T_N were determined by the midpoint of C/T and $d\chi/dT$ jumps. The $T_N(x)$ agrees well with that obtained by the μSR study [13], and gradually decreases with x. This dependence is in contrast to the pressure dependence of T_N with a maximum before the sudden disappearance. This difference should not be explained solely by the effect of disorder because the x dependence of $\rho(T)$ agrees with the pressure dependence of $\rho(T)$ for $CeRu_2Al_{10}$ [2]. Using the detailed pressure dependence of lattice parameters reported recently [14], we have compared the rate of lattice contraction by Fe substitution with that by application of hydrostatic pressure in Fig. 2(e). The room-temperature lattice parameters of $Ce(Ru_{1-x}Fe_x)_2Al_{10}$ were taken from the results obtained

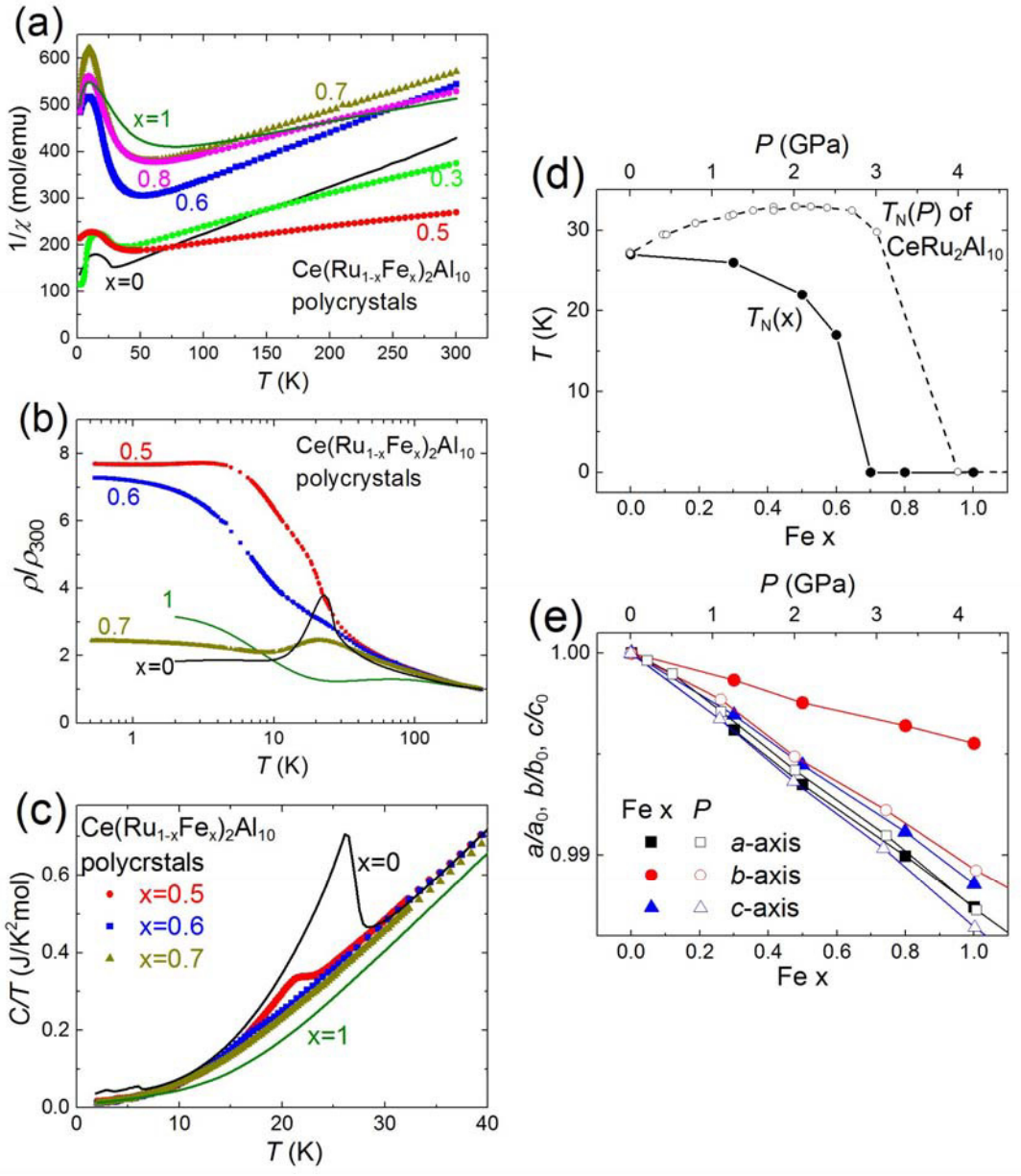

Figure 2: Temperature dependence of (a) inverse magnetic susceptibility, (b) electrical resistivity and (c) specific heat for polycrystalline $Ce(Ru_{1-x}Fe_x)_2Al_{10}$. (d) Magnetic phase diagram of $Ce(Ru_{1-x}Fe_x)_2Al_{10}$ together with the pressure dependence of T_N for $CeRu_2Al_{10}$ [2,8]. (e) Fe concentration dependence of normalized lattice parameters for $Ce(Ru_{1-x}Fe_x)_2Al_{10}$ taken from [13]. Those for $CeRu_2Al_{10}$ under pressure are taken from [14].

by the neutron diffraction [13]. For the comparison, the lattice parameters are normalized by those at $x = 0$ and ambient pressure, respectively. The range of pressure is scaled so that the slopes of a/a_0 coincide each other. Obviously, the contraction rate of *b*-axis, $\Delta b/b$, for Fe substitution is nearly a half of those of $\Delta a/a$ and $\Delta c/c$, while the contraction by hydrostatic pressure is almost isotropic. Therefore, in addition to the effect of disorder, the anisotropic lattice contraction, $\Delta a/a \approx \Delta c/c \approx 2\Delta b/b$, induced by Fe substitution should weaken the unusual antiferromagnetic order of $CeRu_2Al_{10}$. Indeed, the importance of two dimensional character within the *ac* plane has been pointed out by the transport and optical studies [15,16]. Moreover, the importance of anisotropic *c-f* hybridization for the unusual AFM in $CeRu_2Al_{10}$ was argued by many experiments such as the neutron scattering and detailed magnetic-field dependence of χ and ρ [5,17]. Therefore, the instability of AFM order by Fe substitution should originate from the change in *c-f* hybridization anisotropy due to the anisotropic lattice contraction. As another explanation, owing to the anisotropic contraction and disorder, the Fe substitution may prevent the formation of charge-density-wave instability proposed by the optical study [16], which should be experimentally examined further. In order to clarify the role of anisotropic lattice contraction for the unusual AFM order, we plan to study the uniaxial pressure effect on $CeRu_2Al_{10}$.

4 Summary

We have reinvestigated the Fe substitution effect on the unusual AFM order in $CeRu_2Al_{10}$ by using both single- and poly-crystalline samples. Scanning electron images and quantitative analyses of atomic composition indicate that a phase segregation occurs in single-crystalline $Ce(Ru_{1-x}Fe_x)_2Al_{10}$ grown by the Al self-flux method. On the other hand, polycrystalline samples are homogeneous mixture of Ru and Fe whose nominal compositions agree with quantitative analyses. The magnetic susceptibility and electrical resistivity of polycrystalline $Ce(Ru_{1-x}Fe_x)_2Al_{10}$ confirm the enhancement of *c-f* hybridization and suppression of semiconducting behavior above T_N with increasing *x*, which are consistent with the data for single crystals. On the contrary to the peaking in T_N as a function of *x* in single-crystalline $Ce(Ru_{1-x}Fe_x)_2Al_{10}$ and as a function of hydrostatic pressure on $CeRu_2Al_{10}$, T_N shows a gradual decrease with increasing *x* up to $x_C = 0.7$. This contrasting behaviors in T_N should result from the anisotropic lattice contraction observed in $Ce(Ru_{1-x}Fe_x)_2Al_{10}$, which emphasizes the importance of the hybridization along the *b* axis for the unusually high T_N in $CeRu_2Al_{10}$.

Acknowledgements

This work was supported by Grants-in-Aid for Scientific Research (Nos. 23840033 and 26400363) from the Japan Society for the Promotion of Science.

References

[1] A. M. Strydom. Physica B **404** (2009) 2981.
[2] T. Nishioka Y. Kawamura, T. Takesaka, R. Kobayashi, H. Kato, M. Matsumura, K. Kodama, K. Matsubayashi, Y. Uwatoko. J. Phys. Soc. Jpn. **78** (2009) 123705.
[3] Y. Muro, K. Yutani, J. Kajino, T. Takabatake. J. Phys.: Conf. Ser. **391** (2012) 012049.
[4] D. D. Khalyavin, A. D. Hillier, D. T. Adroja, A. M. Strydom, P. Manuel, L. C. Chapon, P. Peratheepan, K. Knight, P. Deen, C. Ritter, Y. Muro, and T. Takabatake. Phys. Rev. B **82** (2010) 100405(R).
[5] J. Robert, J. M. Mignot, S. Petit, P. Steffens, T. Nishioka, R. Kobayashi, M. Matsumura,

H. Tanida, D. Tanaka, M. Sera. Phys. Rev. Lett. **109** (2012) 267208.
[6] V. M. T. Thiede, T. Ebel, W. Jeitschko. J. Mater. Chem. **8** (1998) 125.
[7] G. Morrison, N. Haldoaarachchige, D. P. Young, J. Y. Chan. J. Phys.: Condens. Matter **24** (2012) 356002.
[8] H. Tanida, Y. Nonaka, D. Tanaka, M. Sera, T. Nishioka, M. Matsumura. Phys. Rev. B **86** (2012) 085144.
[9] T. Nishioka, D. Hirai, Y. Kawamura, H. Kato, M. Matsumura, H. Tanida, M. Sera, K. Matsubayashi, Y. Uwatoko. J. Phys.: Conf. Ser. **273** (2011) 012046.
[10] K. Hayashi, Y. Muro, T. Fukuhara, T. Kuwai. JPS Conf. Proc. **3** (2014) 012019.
[11] S. Hoshino, Y. Kuramoto. Phys. Rev. Lett. 111 (2013) 026401.
[12] Y. Zekko, Y. Yamamoto, H. Yamaoka, F. Tajima, T. Nishioka, F. Strigari, A. Severing, J. F. Lin, N. Hiraoka, H. Ishii, K. D. Tsuei, J. Mizuki. Phys. Rev. B **89** (2014) 125108.
[13] D. T. Adroja, A. D. Hillier, Y. Muro, J. Kajino, T. Takabatake, P. Peratheepan, A. M. Strydom, P. P. Deen, F. Demmel, J. R. Stewart, J. W. Taylor, R. I. Smith, S. Ramos, M. A. Adams. Phys. Rev. B **87** (2013) 224415.
[14] Y. Kawamura, T. Kawaai, T. Nakayama, H. Hayashi, K. Takeda, C. Sekine, T. Nishioka, Y. Ohishi. JPS Conf. Proc. **3** (2014) 011029.
[15] H. Tanida, D. Tanaka, M. Sera, C. Moriyoshi, Y. Kuroiwa, T. Takesaka, T. Nishioka, H. Kato, M. Matsumura. J. Phys. Soc. Jpn. **79** (2010) 063709.
[16] S. Kimura, T. Iizuka, H. Miyazaki, T. Hajiri, M. Matsunami, T. Mori, A. Irizawa, Y. Muro, J. Kajino, T. Takabatake. Phys. Rev. B **84** (2011) 165125.
[17] H. Tanida, Y. Nonaka, D. Tanaka, M. Sera, Y. Kawamura, Y. Uwatoko, T. Nishioka, M. Matsumura. Phys. Rev. B **85** (2012) 205208.